ACS Photonics

Article

pubs.acs.org/journal/apchd5

# Quantum Beats in Hybrid Metal–Semiconductor Nanostructures

Chandriker Kavir Dass,[†] Thomas Jarvis,[†,‡] Vasyl P. Kunets,[§] Yuriy I. Mazur,[§] Gregory G. Salamo,[§] Christoph Lienau,[∥] Parinda Vasa,[⊥] and Xiaoqin Li*[,†]

[†]Department of Physics, University of Texas at Austin, Austin, Texas 78712, United States

[§]Institute for Nanoscience and Engineering, University of Arkansas, Fayetteville, Arkansas 72701, United States

[∥]Institut für Physik, Carl von Ossietzky Universität, D-26111 Oldenburg, Germany

[⊥]Department of Physics, Indian Institute of Technology Bombay, Mumbai 400 076, India

Supporting Information

**ABSTRACT:** We investigate nonradiative quantum coherence in the presence of coupling between excitons and surface plasmon polaritons (SPPs) in a hybrid metal–semiconductor nanostructure. In particular, we study how quantum coherence between heavy-hole (HH) and light-hole (LH) excitons in a GaAs quantum well (QW) is modified when they are coupled to SPPs of a gold grating. We find that the nonradiative coherence is reduced in correlation with the coupling strength between the excitons and SPPs. Under the resonant coupling condition, the nonradiative coherence remains in the range of hundreds of femtoseconds, which is significantly longer than the plasmonic coherence. These experiments directly probe quantum dynamics in a prototypical hybrid system and provide critical information for exploring future quantum plasmonics applications.

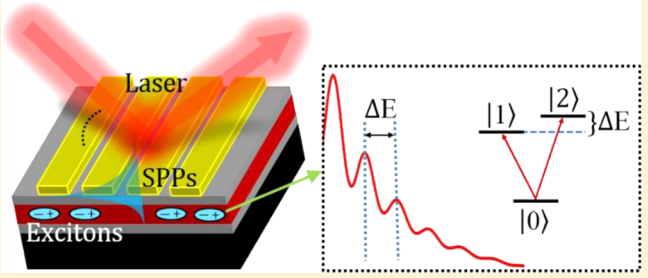


**KEYWORDS:** *plasmonics, quantum well, hybrid nanostructure, ultrafast spectroscopy, quantum coherence*

Coherent superposition of two or multiple quantum states, which are not dipole coupled, is known as nonradiative quantum coherence. Such coherence plays an essential role in a host of novel phenomena such as lasing without inversion,[1−3] electromagnetically induced transparency,[4,5] and entanglement.[6,7] These phenomena have been investigated extensively in atomic and solid state systems, especially motivated by interest in controlling and manipulating individual quantum systems for quantum information processing.[8−13] In some cases it is sufficient to describe the phenomena with a few-level model coupled to a coherent driving field. In other cases (e.g., in semiconductors), many-body interactions among optically excited quasiparticles need to be taken into account to gain a comprehensive, microscopic understanding. For example, the studies of quantum beats between excitons in semiconductor quantum wells (QWs) have provided much insight into the coherent interaction and quantum dynamics of a canonical many-body system.[6,14−17]

In a different context, plasmonics has emerged in the last two decades as a promising approach for concentrating and manipulating light at subwavelength dimensions. Hybrid structures that combine the metal-based plasmonic nanostructures and semiconductor-based photonic components are particularly interesting because such hybrid structures take advantage of both material platforms to achieve optical gain and nonlinear signal modulation with a smaller device footprint. To this end, novel devices such as compact all-optical switches,[18−20] single-photon transistors,[21] and nanolasers[22−24] based on hybrid nanostructures have been demonstrated. To achieve rational device design, it is essential to understand how electronic and photonic coupling between the components modify the ultrafast and quantum dynamics of the fundamental optical excitations, that is, excitons and SPPs in hybrid structures.

While a number of experiments have demonstrated exciton and plasmonic coupling effects,[25−28] few previous studies have investigated how quantum coherence is modified in hybrid structures.[29] The decoherence time, or dephasing time, determines the time scale during which electrons or quasiparticles can be manipulated coherently by light and, thus, is a particularly critical parameter for optoelectronic devices. Very fast dephasing times of plasmonic resonances, on the order of tens of femtoseconds, have been reported in metallic nanostructures,[30−32] while the dephasing times of excitons in semiconductors and their heterostructures can be rather long. In QWs, the exciton dephasing time lasts a few picoseconds to tens of picoseconds at low temperatures,[33−35] and this dephasing time is further extended close to a nanosecond in quantum dots.[36−38] In this work, we aim to answer the question whether the fast dephasing time of the metallic nanostructure becomes the limiting factor in a hybrid structure. This information is particularly critical for quantum

**Received:** June 15, 2015
**Published:** August 4, 2015





DOI: 10.1021/acsphotonics.5b00328
*ACS Photonics* 2015, 2, 1341−1347

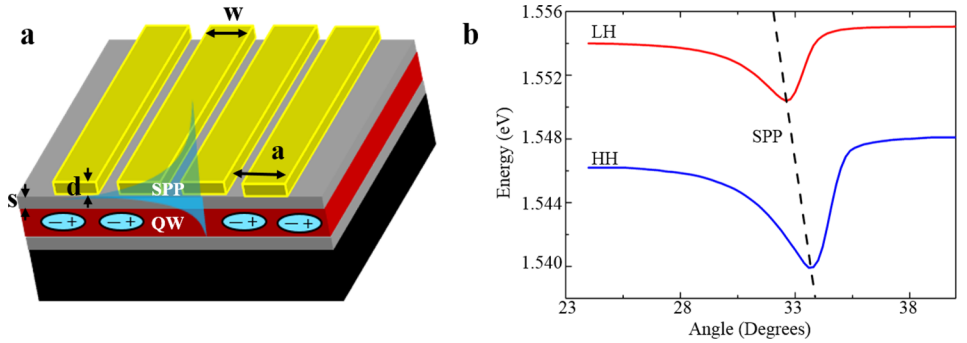


**Figure 1.** (a) Schematic of the hybrid structure. The grating structure has period ($a$ = 500 nm), thickness ($d$ = 80 nm), grating/well separation ($s$ = 20 nm), and width ($w$ = 140 nm). (b) Simulated linear dispersion of LH and HH resonances in the presence of exciton−SPP coupling at ∼10 K. The black dashed line marks the uncoupled dispersion of the SPP mode composed of air−metal and semiconductor−metal SPPs. The simulation reveals a clear shift of the LH and HH QW resonances at an angle of ∼34°.

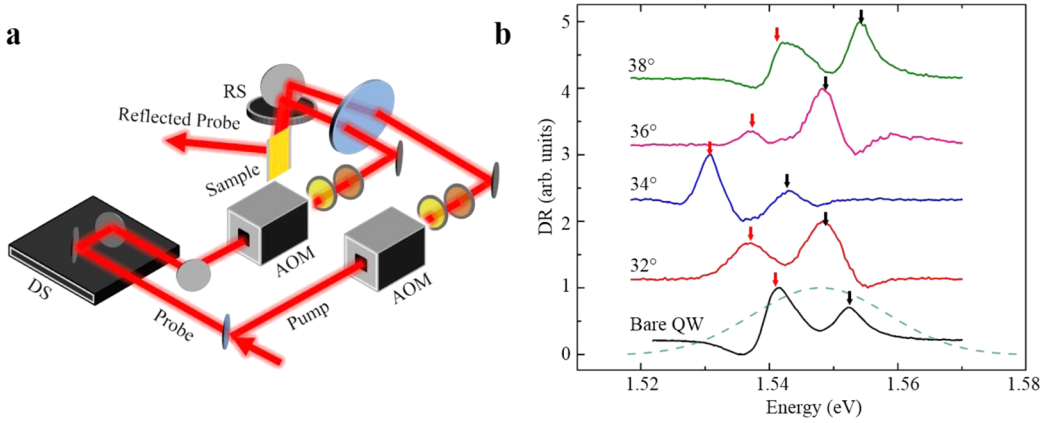


**Figure 2.** (a) Schematic of the experimental setup. The pump−probe delay is controlled with a delay stage (DS). Both pump and probe are modulated in intensity with AOMs. Linear polarizers and $\lambda/2$ waveplates are placed after the AOMs for power and polarization control. A rotation stage is used to vary the incidence angle onto the sample, after which the reflected probe is collected. (b) Spectrally resolved DR on the bare QW and the hybrid structure at ∼10 K. The red (black) arrows indicate the positions of the HH (LH) resonances and the blue dashed curve shows the excitation laser. Spectra at four different incidence angles are measured on the hybrid structure, showing a clear shift in the LH−HH exciton resonances.

plasmonics, an emerging frontier aiming to address challenges in quantum communication and quantum information processing.[21,39−42]

Here, we report an experimental study of the nonradiative coherence between heavy-hole (HH) and light-hole (LH) excitons in a metal−semiconductor hybrid structure consisting of a gold grating in close proximity to a GaAs/AlGaAs QW. This nonradiative coherence has been referred to as Raman coherence in previous studies[7,14] and often manifests itself as a quantum beat in nonlinear pump−probe experiments or photoluminescence.[14,15] The investigated hybrid structure is designed to optimize the radiative exciton−SPP interaction. We study the modification of Raman coherence by exciton−SPP coupling using low-temperature, angle-resolved, far-field differential reflection (DR) spectroscopy. As a result of the coupling, a significant resonance energy shift of ∼7 meV has been observed. By studying the time scale over which quantum beats decay, we find that the nonradiative coherence time for the hybrid system decreases in correlation with the exciton−SPP coupling strength. Our investigation reveals that the nonradiative coherence remains in the range of hundreds of femtoseconds, which is significantly longer than the plasmonic coherence. These studies shed light on coherent dynamics in hybrid materials essential for exploring future quantum plasmonic applications.

The sample investigated is a metal−semiconductor hybrid structure (see Figure 1a) consisting of a gold grating structure fabricated on top of an AlGaAs/GaAs QW. The AlGaAs/GaAs QW consists of a 10 nm GaAs well embedded between $Al_{0.3}Ga_{0.7}As$ barriers grown on top of a GaAs substrate by molecular beam epitaxy (MBE). The gold grating and GaAs QW are placed in close proximity (with a 20 nm separation) to enable coupling between excitons and SPPs. The grooves, fabricated by e-beam lithography, have a thickness of 80 nm, a width of 140 nm, and a period of 500 nm. When such a hybrid structure is illuminated with p-polarized light, with its electric field vector perpendicular to the grooves, SPPs are excited at both air−metal (AM) and semiconductor−metal (SM) interfaces by transferring momentum ($n2\pi/a$) to the incident photons, where $n$ is an integer and $a$ is the grating period. The SPP field at the SM interface is mostly evanescent, with a decay length of only ∼50 nm due to the large dielectric constant of the semiconductor. When placed within this decay length, the QW excitons couple to the strong evanescent plasmonic field. The hybrid structure parameters are chosen such that, at an incidence angle of 34°, the HH and LH exciton resonances of the QW at a temperature of 10 K, occurring at 1.531 eV (810


DOI: 10.1021/acsphotonics.5b00328
ACS Photonics 2015, 2, 1341−1347

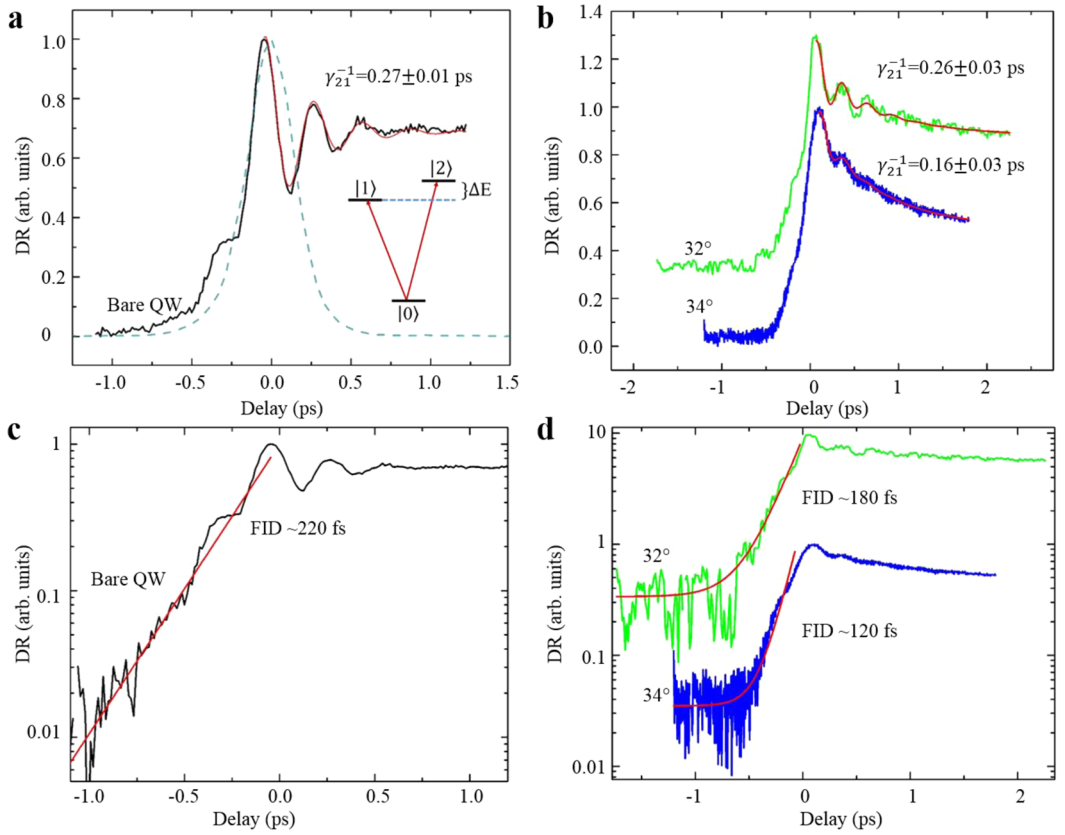


**Figure 3.** (a) Time-resolved DR for the bare QW (black trace) and the fit (red trace) to eq 1. The inset shows a schematic V-level system, which is used to derive eq 1. |1⟩, |2⟩, and |0⟩ represent the HH, LH exciton, and ground state, respectively. The pulse duration is shown by the blue dashed curve. (b) Time-resolved DR for the hybrid structure at two different incidence angles and fits (red traces) to eq 1. At the resonant coupling angle of 34° (blue trace), a marked decrease in the Raman coherence is seen compared to the bare QW. At 32° (green trace), a noticeable, but smaller decrease is seen in the Raman coherence. (c) Log-scale, time-resolved DR for the bare QW (black trace). An exponential decay fit (red trace) is shown for the negative delay. (d) Log-scale, time-resolved DR for the hybrid structure at 34° (blue trace), 32° (green trace), and exponential decay fits (red traces) for the negative delays.

nm) and 1.543 eV (803 nm), match well with the three coupled SPP modes: AM[$n = -1$], SM[$n = +2$], and SM[$n = -3$]. This design also ensures an efficient groove-induced coupling of the incident light to evanescent SPP fields and makes it possible to probe the hybrid structure response by far-field measurements. The highly angle-dependent AM SPP, and the almost angle-independent QW exciton, provide an efficient way to control the interaction between SPPs and excitons by angle-tuning. The grating structure covers a region of approximately 200 $\mu$m by 200 $\mu$m on the sample and is surrounded by regions of the bare QW, allowing us to probe the hybrid structure as well as the bare QW.

Here, we briefly describe the coupling mechanism between excitons and SPPs in the hybrid nanostructure, which has been discussed carefully in our earlier work.[27] To explain the SPP–exciton interaction, a phenomenological model, treating the exciton and SPP resonances as complex Lorentzian oscillators, has proven successful. As a first approximation, the SPP coupling of HH and LH excitons is treated separately because of their sufficiently different energies. Such a phenomenological model correctly predicts various features of the optical response.[27] Most importantly, it reproduces the large spectral red shift of the exciton resonance observed when increasing the incidence angle toward 34° and the concomitant change in the radiative damping of the exciton resonances. The largely asymmetric spectral shifts below and above 34° have been assigned to the constructive and destructive interference between the interacting SPP modes. This well-studied linear optical response is mainly governed by the coupling of excitonic dipole moments to vacuum fluctuations of the SPP modes of the grating.[27] Due to this coupling, the exciton and SPP resonances are transformed into higher and lower energy exciton–SPP polariton modes, exhibiting significantly altered dispersion relations as shown in the simulations presented in Figure 1b.

The homodyne detected, pump–probe (or DR) experiment is shown schematically in Figure 2a. The excitation source is a Ti:sapphire oscillator that produces pulses of ~150 fs at a 78 MHz repetition rate. The laser is split into a pump and probe beam whose intensities are modulated by acousto-optic modulators (AOMs) at a frequency of 0.5 and 0.515 MHz, respectively. The DR signal is extracted from a lock-in amplifier at the difference frequency of 15 kHz between the pump and probe modulation frequencies. After the AOMs, each beam passes through a $\lambda/2$ waveplate and a linear polarizer for power and polarization control. All measurements presented in this paper are performed at a temperature of ~10 K with $p$-polarization to ensure resonant SPP excitation. A delay stage (DS) in the probe path is used to control the relative delay between the two beams. The two beams are focused onto the sample at angles variable via a mirror mounted on a rotation


DOI: 10.1021/acsphotonics.5b00328
ACS Photonics 2015, 2, 1341–1347

stage (RS). The reflected probe is then sent through a spectrometer and onto a single-channel photodetector.

We begin with investigating the response of the hybrid nanostructure by angular and spectrally resolved measurements to confirm the calculated resonant coupling conditions. Pump−probe spectra taken near zero delay at four different incidence angles on the hybrid structure, as well as on the bare QW, are displayed in Figure 2b. The spectrum at 34° incidence angle shows a clear red-shift of ∼7 meV for both the HH and LH excitons due to their dipole-coupling to SPP modes. Spectra taken at other angles show reduced spectral shifts in comparison to the spectrum taken on the bare QW. Thus, we conclude that the strongest exciton−plasmon coupling occurs at ∼34°, consistent with the plasmonic grating design and previous studies.[27] In addition, the signal strengths from the hybrid structure are comparable to those from the bare QW, from which we ascertain no significant change in the optical quality of the QW due to grating fabrication. We also observe a slight angle dependence of the LH and HH resonance widths, indicating that the coupling to SPPs modifies the radiative damping of the exciton resonances.[27,29] Comparison to model calculations indicates that the line shapes of these resonances can only be fully explained by including several physical effects simultaneously, specifically excitation-induced dephasing, inhomogeneous broadening, and pump-induced spectral shifts.[43−45] The combination of these effects can lead to large phase changes and asymmetries in the individual resonance line shapes. In the context of the present paper, we only focus on extracting an estimated resonance energy shift to confirm exciton−SPP coupling.

We now turn to study the quantum beats between HH and LH excitons in the bare QW as a reference. The experiments were performed at 34° incidence angle to facilitate comparison to the hybrid system. The central wavelength of the excitation laser is tuned to 1.55 eV with a full width half-maximum (fwhm) of 21 meV. The laser spectrum is broad enough to excite both the HH and LH excitons simultaneously. The nonlinear signal copropagating with the probe beam is first sent through the spectrometer centered at the LH exciton resonance before reaching the photodetector. As the delay between the pump/probe beams is varied, we observe a pronounced oscillatory signal with decaying amplitude, as shown in Figure 3a. Such beating signals have been observed in earlier studies on QWs and are assigned to quantum beats between the HH and LH excitons in the quantum well.[46,47] The DR signal is fit to the following expression:

$$\mathrm{DR}(\tau) \propto Ae^{-\Gamma\tau} + Be^{-\gamma_{21}\tau}\cos(\omega_{21}\tau) \qquad (1)$$

where $\Gamma$ describes the population relaxation rate of the LH exciton, $\gamma_{21}$ is the dephasing rate for the Raman coherence between HH and LH excitons, and $A$ and $B$ are amplitude coefficients. In the absence of inhomogeneous broadening, the Raman coherence is determined by the population decay of both HH and LH resonances (given by population relaxation rates $\Gamma_{01}$ and $\Gamma_{02}$, respectively) and an additional pure dephasing term $\gamma_{21}^{\mathrm{pure}}$. The dephasing rate can then be written as $\gamma_{21} = (1/2)(\Gamma_{01} + \Gamma_{02}) + \gamma_{21}^{pure}$. The oscillation period ($T_R$) is inversely proportional to the LH−HH energy splitting ($\Delta E = \hbar\omega_{21}$) by $T_R\omega_{21} = 2\pi$. The derivation of this fitting function, in terms of the optical Bloch equation, is described in the Supporting Information. In the presence of strong inhomogeneous broadening, the exponential damping term $e^{-\gamma_{21}\tau}$ in eq 1 should be replaced by $e^{-\gamma_{21}\tau}e^{-\tau^2/(2\sigma^2)}$, where $\sigma$ corresponds to the inhomogeneous line width.[48]

We analyze the quantum beats measured on the bare QW by fitting the data using eq 1, which yields $\gamma_{21}^{-1} = 0.27 \pm 0.01$ ps and $T_R = 0.152 \pm 0.001$ ps for the Raman coherence time and oscillation period, respectively. No population decay is measurable even on a time scale as long as 20 ps. In QWs, it is known that this long decay time does not reflect the population decay time of the optically excited bright excitons, but rather the average lifetime of a thermalized ensemble of bright and dark excitons, populated by scattering from bright to dark excitons.[49−52] Even though a direct measurement of the bright exciton population relaxation time is not straightforward,[53] it is understood that such relaxation times are in the range of a few picoseconds. Therefore, the observed value of $\gamma_{21}^{-1} = 0.27 \pm 0.01$ ps in our sample mainly reflects the inhomogeneous broadening of the QW resonances. The oscillation period determined from the fitting corresponds to a LH−HH splitting of ∼27 meV. This value agrees with the LH−HH exciton splitting (∼30 meV) estimated from the spectrum within experimental uncertainties since the inhomogeneous broadening of the exciton resonances affects the estimate of the energy splitting determined from the spectrum.

Next, we perform experiments on the hybrid structure at 34° incidence angle, which satisfies the exciton−SPP resonant coupling condition. As shown in Figure 3b, we observe significantly reduced Raman coherence time as well as an apparent LH exciton population decay. The fitting, using eq 1, yields values of $T_R = 0.134 \pm 0.005$ ps, $\Gamma^{-1} = 0.70 \pm 0.03$ ps, and $\gamma_{21}^{-1} = 0.16 \pm 0.03$ ps. The beat period has reduced due to the coupling dependent redshift of the HH and LH resonances, which increases the LH−HH separation to 31 meV. The population relaxation time has decreased significantly due to the Purcell effect, that is, the excitons couple to the increased photonic density of states near the grating. This observation is consistent with the reduced exciton lifetime near plasmonic structures previously reported by many groups.[27,54−56] For such gratings, earlier work has also shown that the radiative damping of the plasmon excitation dominates over Ohmic loss.[57] Hence, the population relaxation rate is now limited by radiative relaxations in agreement with the observed broadening of dressed exciton resonances beyond the inhomogeneous broadening.[29,58,59] The Raman coherence time is directly related to the HH and LH population relaxation and, thus, is reduced by almost a factor of 2 in the presence of exciton−plasmon coupling. Pure dephasing and inhomogeneous broadening still plays a partial, but reduced, role in determining the Raman coherence in comparison to the case of bare QW. Interestingly, the Raman coherence in the hybrid system is almost an order of magnitude longer than the quantum coherence of the SPP resonance, which is estimated to be tens of femtoseconds as suggested by its broad homogeneous line width. Thus, in this type of hybrid structure, the SPPs may significantly enhance the light out-coupling efficiency without severely limiting the coherence time.

Yet, there may be an alternative explanation to our results. It is known that many-body interactions between excitons leads to excitation induced dephasing, that is, a reduction of quantum coherence time at higher exciton density.[44] One may argue that the reduced Raman coherence time in the hybrid structure may arise from the enhanced local electric-field near the plasmonic grating, leading to more pronounced excitation induced dephasing than the case of the bare QW. To test this



DOI: 10.1021/acsphotonics.5b00328
ACS Photonics 2015, 2, 1341−1347

alternative explanation, we perform additional measurements at an incidence angle of 32°, which is near the resonant coupling angle. At this angle, the local field strength at the QW is nearly identical to that at 34° incidence angle.[45] As shown in Figure 3b, there is clearly a difference between the quantum beats measured at these two incidence angles. The fitting using eq 1 to the quantum beats at 32° incidence angle yields time scales of $\Gamma^{-1} = 0.76 \pm 0.06$ ps, $\gamma_{21}^{-1} = 0.26 \pm 0.03$ ps, and $T_R = 0.144 \pm 0.003$ ps. Raman coherence extracted for 32° incidence angle is clearly longer than that extracted at 34°, although the local E-field is nearly the same. This observation demonstrates that the reduction of the Raman coherence time correlates with the coupling strength between excitons and SPPs.

Additional information can be obtained by examining the dynamics during the negative delay, as shown in Figure 3c,d. At negative time delays, the probe pulse arrives first and induces a LH polarization coherence, which subsequently goes through free induction decay (FID). We obtain a dephasing time for the LH exciton by fitting an exponential function to the decay during the negative delay in Figure 3c,d, which yields a time scale of about 220, 180, and 120 fs for the case of the bare QW and the hybrid structure at 32° and 34° incidence angles, respectively. Although Raman coherence time is not directly given by exciton dephasing time (i.e., Raman coherence time can be longer than exciton dephasing time), both time scales are affected by population relaxation processes and change systematically in the bare QW and the hybrid structure. Oscillatory signals during negative time delay have also been observed in Figure 3. Such oscillatory signals at negative delays have been attributed to a number of possible mechanisms including superposition of the HH and LH free induction decay, many body effects from exciton−exciton interaction or higher order (e.g., fifth order) nonlinear signals in previous studies on bare QWs.[16,60]

In summary, we have investigated quantum coherent dynamics in a prototypical hybrid structure consisting of a semiconductor QW coupled to a metallic plasmonic grating. Interestingly, even though the exciton resonances are predominantly inhomogeneously broadened in the bare QW, the coupling to SPPs significantly affects the coherent dynamics of the system. Our work demonstrates that the coupling between excitons and SPPs provides an opportunity to control nonradiative quantum coherence in a hybrid system. In the structure investigated, the coupling strength between excitons and plasmons is moderate. In future work, one may explore hybrid systems in the strong coupling limit by decreasing the thickness of the barrier between the QW and plasmonic structures or reducing inhomogeneous broadening of excitons and the plasmonic resonance line width using a different design other than a grating. In case of sufficiently strong coupling, the modified radiative relaxation rate can be either enhanced or suppressed by the constructive or the destructive interference between the exciton and SPP modes controllable via their distance. While we report enhanced radiative relaxation due to Purcell effect and constructive interference of the modes here, destructive interference leads to a drastically different phenomenon. In the case of destructive interference, the hybrid exciton−SPP mode is completely decoupled from the environment leading to the total suppression of the spontaneous emission or the population trapping, resulting in an extremely long coherence time. It is a situation analogous to the electromagnetically induced transparency but entirely induced by the fluctuating vacuum field.[4,61−63] Controlling such quantum coherence may provide a promising approach to designing active quantum plasmonic devices.

## ■ ASSOCIATED CONTENT

### Supporting Information

Outline of the solution to the optical Bloch equation for a three-level "V" system used to derive eq 1. The Supporting Information is available free of charge on the ACS Publications website at DOI: 10.1021/acsphotonics.5b00328.

(PDF)

## ■ AUTHOR INFORMATION


### Corresponding Author

*E-mail: elaineli@physics.utexas.edu.

### Present Address

‡Department of Physics and Astronomy, Bates College, Lewiston, Maine 04240, U.S.A.


### Notes

The authors declare no competing financial interest.

## ■ ACKNOWLEDGMENTS

The work at UT-Austin is supported by NSF DMR-1306878, and Welch Foundation F-1662 and at UA-Fayetteville is supported by NSF DMR-1309989 and NSF EPSCoR-EPS1003970. C.L. and P.V. thank the Deutsche Forschungsgemeinschaft (SPP 1391 and DFG-NSF Materials World Network), and the Korea Foundation for International Cooperation of Science and Technology (Global Research Laboratory Project, K20815000003) for financial support. X.L. also gratefully acknowledges the support from a Humboldt fellowship.

## ■ REFERENCES


(1) Scully, M. O.; Zhu, S.; Gavrielides, A. Degenerate Quantum-Beat Laser: Lasing without Inversion and Inversion without Lasing. *Phys. Rev. Lett.* **1989**, *62*, 2813.

(2) Harris, S. E. Lasers without Inversion: Interference of Lifetime-Broadened Resonances. *Phys. Rev. Lett.* **1989**, *62*, 1033.

(3) Scully, M. O. Resolving Conundrums in Lasing without Inversion Via Exact Solutions to Simple Models. *Quantum Opt.* **1994**, *6*, 203.

(4) Boller, K.-J.; Imamoglu, A.; Harris, S. E. Observation of Electromagnetically Induced Transparency. *Phys. Rev. Lett.* **1991**, *66*, 2593.

(5) Field, J. E.; Hahn, K. H.; Harris, S. E. Observation of Electromagnetically Induced Transparency in Collisionally Broadened Lead Vapor. *Phys. Rev. Lett.* **1991**, *67*, 3062.

(6) Lenihan, A. S.; Dutt, M. V.; Steel, D. G.; Ghosh, S.; Bhattacharya, P. K. Raman Coherence Beats from Entangled Polarization Eigenstates in InAs Quantum Dots. *Phys. Rev. Lett.* **2002**, *88*, 223601.

(7) Li, X.; Wu, Y.; Steel, D. G.; Gammon, D.; Sham, L. J. Raman Coherence Beats from the Entangled State Involving Polarized Excitons in Single Quantum Dots. *Phys. Rev. B: Condens. Matter Mater. Phys.* **2004**, *70*, 195330.

(8) Chen, P.; Piermarocchi, C.; Sham, L. J. Control of Exciton Dynamics in Nanodots for Quantum Operations. *Phys. Rev. Lett.* **2001**, *87*, 067401.

(9) Troiani, F.; Hohenester, U.; Molinari, E. Exploiting Exciton-Exciton Interactions in Semiconductor Quantum Dots for Quantum-Information Processing. *Phys. Rev. B: Condens. Matter Mater. Phys.* **2000**, *62*, R2263.

(10) Liu, C.; Dutton, Z.; Behroozi, C. H.; Hau, L. V. Observation of Coherent Optical Information Storage in an Atomic Medium Using Halted Light Pulses. *Nature* **2001**, *409*, 490−493.




DOI: 10.1021/acsphotonics.5b00328
*ACS Photonics* 2015, 2, 1341−1347

(11) Hald, J.; Sørensen, J. L.; Schori, C.; Polzik, E. S. Spin Squeezed Atoms: A Macroscopic Entangled Ensemble Created by Light. *Phys. Rev. Lett.* **1999**, *83*, 1319−1322.
(12) Xu, Q.; Sandhu, S.; Povinelli, M. L.; Shakya, J.; Fan, S.; Lipson, M. Experimental Realization of an on-Chip All-Optical Analogue to Electromagnetically Induced Transparency. *Phys. Rev. Lett.* **2006**, *96*, 123901.
(13) Barenco, A.; Deutsch, D.; Ekert, A.; Jozsa, R. Conditional Quantum Dynamics and Logic Gates. *Phys. Rev. Lett.* **1995**, *74*, 4083.
(14) Ferrio, K. B.; Steel, D. G. Raman Quantum Beats of Interacting Excitons. *Phys. Rev. Lett.* **1998**, *80*, 786.
(15) Langer, V.; Stolz, H.; von der Osten, W. Observation of Quantum Beats in the Resonance Fluorescence of Free Excitons. *Phys. Rev. Lett.* **1990**, *64*, 854.
(16) Leo, K.; Shah, J.; Göbel, E. O.; Damen, T. C.; Schmitt-Rink, S.; Schäfer, W.; Köhler, K. Coherent Oscillations of a Wave Packet in a Semiconductor Double-Quantum-Well Structure. *Phys. Rev. Lett.* **1991**, *66*, 201.
(17) Flissikowski, T.; Hundt, A.; Lowisch, M.; Rabe, M.; Henneberger, F. Photon Beats from a Single Semiconductor Quantum Dot. *Phys. Rev. Lett.* **2001**, *86*, 3172.
(18) Dintinger, J.; Robel, I.; Kamat, P. V.; Genet, C.; Ebbesen, T. W. Terahertz All-Optical Molecule-Plasmon Modulation. *Adv. Mater.* **2006**, *18*, 1645−1648.
(19) MacDonald, K. F.; Samson, Z. L.; Stockman, M. I.; Zheludev, N. I. Ultrafast Active Plasmonics. *Nat. Photonics* **2009**, *3*, 55−58.
(20) Vasa, P.; Pomraenke, R.; Cirmi, G.; De Re, E.; Wang, W.; Schwieger, S.; Leipold, D.; Runge, E.; Cerullo, G.; Lienau, C. Ultrafast Manipulation of Strong Coupling in Metal− Molecular Aggregate Hybrid Nanostructures. *ACS Nano* **2010**, *4*, 7559−7565.
(21) Chang, D. E.; Sorensen, A. S.; Demler, E. A.; Lukin, M. D. A Single-Photon Transistor Using Nanoscale Surface Plasmons. *Nat. Phys.* **2007**, *3*, 807−812.
(22) Oulton, R. F.; Sorger, V. J.; Zentgraf, T.; Ma, R.; Gladden, C.; Dai, L.; Bartal, G.; Zhang, X. Plasmon Lasers at Deep Subwavelength Scale. *Nature* **2009**, *461*, 629−632.
(23) Bergman, D. J.; Stockman, M. I. Surface Plasmon Amplification by Stimulated Emission of Radiation: Quantum Generation of Coherent Surface Plasmons in Nanosystems. *Phys. Rev. Lett.* **2003**, *90*, 027402.
(24) Lu, Y.; Kim, J.; Chen, H.; Wu, C.; Dabidian, N.; Sanders, C. E.; Wang, C.; Lu, M.; Li, B.; Qiu, X. Plasmonic Nanolaser Using Epitaxially Grown Silver Film. *Science* **2012**, *337*, 450−453.
(25) Bellessa, J.; Bonnand, C.; Plenet, J. C.; Mugnier, J. Strong Coupling between Surface Plasmons and Excitons in an Organic Semiconductor. *Phys. Rev. Lett.* **2004**, *93*, 036404.
(26) Vasa, P.; Wang, W.; Pomraenke, R.; Lammers, M.; Maiuri, M.; Manzoni, C.; Cerullo, G.; Lienau, C. Real-Time Observation of Ultrafast Rabi Oscillations between Excitons and Plasmons in Metal Nanostructures with J-Aggregates. *Nat. Photonics* **2013**, *7*, 128−132.
(27) Vasa, P.; Pomraenke, R.; Schwieger, S.; Mazur, Y. I.; Kunets, V.; Srinivasan, P.; Johnson, E.; Kihm, J. E.; Kim, D. S.; Runge, E. Coherent Exciton−Surface-Plasmon-Polariton Interaction in Hybrid Metal-Semiconductor Nanostructures. *Phys. Rev. Lett.* **2008**, *101*, 116801.
(28) Gómez, D. E.; Vernon, K. C.; Mulvaney, P.; Davis, T. J. Surface Plasmon Mediated Strong Exciton−Photon Coupling in Semiconductor Nanocrystals. *Nano Lett.* **2010**, *10*, 274−278.
(29) Wang, W.; Vasa, P.; Pomraenke, R.; Vogelgesang, R.; De Sio, A.; Sommer, E.; Maiuri, M.; Manzoni, C.; Cerullo, G.; Lienau, C. Interplay between Strong Coupling and Radiative Damping of Excitons and Surface Plasmon Polaritons in Hybrid Nanostructures. *ACS Nano* **2014**, *8*, 1056−1064.
(30) Link, S.; El-Sayed, M. A. Spectral Properties and Relaxation Dynamics of Surface Plasmon Electronic Oscillations in Gold and Silver Nanodots and Nanorods. *J. Phys. Chem. B* **1999**, *103*, 8410−8426.
(31) Voisin, C.; Del Fatti, N.; Christofilos, D.; Vallée, F. Ultrafast Electron Dynamics and Optical Nonlinearities in Metal Nanoparticles. *J. Phys. Chem. B* **2001**, *105*, 2264−2280.
(32) Sönnichsen, C.; Franzl, T.; Wilk, T.; von Plessen, G.; Feldmann, J.; Wilson, O.; Mulvaney, P. Drastic Reduction of Plasmon Damping in Gold Nanorods. *Phys. Rev. Lett.* **2002**, *88*, 077402.
(33) Schultheis, L.; Honold, A.; Kuhl, J.; Köhler, K.; Tu, C. W. Optical Dephasing of Homogeneously Broadened Two-Dimensional Exciton Transitions in Gaas Quantum Wells. *Phys. Rev. B: Condens. Matter Mater. Phys.* **1986**, *34*, 9027.
(34) Webb, M. D.; Cundiff, S. T.; Steel, D. G. Observation of Time-Resolved Picosecond Stimulated Photon Echoes and Free Polarization Decay in Gaas/Algaas Multiple Quantum Wells. *Phys. Rev. Lett.* **1991**, *66*, 934−937.
(35) Singh, R.; Autry, T. M.; Nardin, G.; Moody, G.; Li, H.; Pierz, K.; Bieler, M.; Cundiff, S. T. Anisotropic Homogeneous Linewidth of the Heavy-Hole Exciton in (110)-Oriented Gaas Quantum Wells. *Phys. Rev. B: Condens. Matter Mater. Phys.* **2013**, *88*, 045304.
(36) Birkedal, D.; Leosson, K.; Hvam, J. M. Long Lived Coherence in Self-Assembled Quantum Dots. *Phys. Rev. Lett.* **2001**, *87*, 227401.
(37) Borri, P.; Langbein, W.; Schneider, S.; Woggon, U.; Sellin, R. L.; Ouyang, D.; Bimberg, D. Ultralong Dephasing Time in Ingaas Quantum Dots. *Phys. Rev. Lett.* **2001**, *87*, 157401.
(38) Bayer, M.; Forchel, A. Temperature Dependence of the Exciton Homogeneous Linewidth in Ingaas\Gaas Self-Assembled Quantum Dots. *Phys. Rev. B: Condens. Matter Mater. Phys.* **2002**, *65*, 041308.
(39) Huck, A.; Smolka, S.; Lodahl, P.; Sørensen, A. S.; Boltasseva, A.; Janousek, J.; Andersen, U. L. Demonstration of Quadrature-Squeezed Surface Plasmons in a Gold Waveguide. *Phys. Rev. Lett.* **2009**, *102*, 246802.
(40) Akimov, A. V.; Mukherjee, A.; Yu, C. L.; Chang, D. E.; Zibrov, A. S.; Hemmer, P. R.; Park, H.; Lukin, M. D. Generation of Single Optical Plasmons in Metallic Nanowires Coupled to Quantum Dots. *Nature* **2007**, *450*, 402−406.
(41) Altewischer, E.; Van Exter, M. P.; Woerdman, J. P. Plasmon-Assisted Transmission of Entangled Photons. *Nature* **2002**, *418*, 304−306.
(42) Huck, A.; Kumar, S.; Shakoor, A.; Andersen, U. L. Controlled Coupling of a Single Nitrogen-Vacancy Center to a Silver Nanowire. *Phys. Rev. Lett.* **2011**, *106*, 096801.
(43) Shacklette, J. M.; Cundiff, S. T. Role of Excitation-Induced Shift in the Coherent Optical Response of Semiconductors. *Phys. Rev. B: Condens. Matter Mater. Phys.* **2002**, *66*, 045309.
(44) Wang, H.; Ferrio, K.; Steel, D. G.; Hu, Y. Z.; Binder, R.; Koch, S. W. Transient Nonlinear Optical Response from Excitation Induced Dephasing in Gaas. *Phys. Rev. Lett.* **1993**, *71*, 1261.
(45) Vasa, P.; Wang, W.; Pomraenke, R.; Maiuri, M.; Manzoni, C.; Cerullo, G.; Lienau, C. Optical Stark Effects in J-Aggregate−Metal Hybrid Nanostructures Exhibiting a Strong Exciton−Surface-Plasmon-Polariton Interaction. *Phys. Rev. Lett.* **2015**, *114*, 036802.
(46) Leo, K.; Damen, T. C.; Shah, J.; Göbel, E. O.; Köhler, K. Quantum Beats of Light Hole and Heavy Hole Excitons in Quantum Wells. *Appl. Phys. Lett.* **1990**, *57*, 19−21.
(47) Feuerbacher, B. F.; Kuhl, J.; Eccleston, R.; Ploog, K. Quantum Beats between the Light and Heavy Hole Excitons in a Quantum Well. *Solid State Commun.* **1990**, *74*, 1279−1283.
(48) Wang, W.; Vasa, P.; Sommer, E.; De Sio, A.; Gross, P.; Vogelgesang, R.; Lienau, C. Observation of Lorentzian Lineshapes in the Room Temperature Optical Spectra of Strongly Coupled Jaggregate/Metal Hybrid Nanostructures by Linear Two-Dimensional Optical Spectroscopy. *J. Opt.* **2014**, *16*, 114021.
(49) Vinattieri, A.; Shah, J.; Damen, T. C.; Kim, D. S.; Pfeiffer, L. N.; Maialle, M. Z.; Sham, L. J. Exciton Dynamics in Gaas Quantum Wells under Resonant Excitation. *Phys. Rev. B: Condens. Matter Mater. Phys.* **1994**, *50*, 10868−10879.
(50) Munoz, L.; Pérez, E.; Vina, L.; Ploog, K. Spin Relaxation in Intrinsic Gaas Quantum Wells: Influence of Excitonic Localization. *Phys. Rev. B: Condens. Matter Mater. Phys.* **1995**, *51*, 4247.
(51) Vinattieri, A.; Shah, J.; Damen, T. C.; Kim, D. S.; Pfeiffer, L. N.; Sham, L. J. Picosecond Dynamics of Resonantly-Excited Excitons in Gaas Quantum Wells. *Solid State Commun.* **1993**, *88*, 189−193.


DOI: 10.1021/acsphotonics.5b00328
*ACS Photonics* 2015, 2, 1341−1347

(52) Vinattieri, A.; Shah, J.; Damen, T. C.; Goossen, K. W.; Pfeiffer, L. N.; Maialle, M. Z.; Sham, L. J. Electric Field Dependence of Exciton Spin Relaxation in Gaas/Algaas Quantum Wells. *Appl. Phys. Lett.* **1993**, *63*, 3164−3166.
(53) Deveaud, B.; Clérot, F.; Roy, N.; Satzke, K.; Sermage, B.; Katzer, D. S. Enhanced Radiative Recombination of Free Excitons in Gaas Quantum Wells. *Phys. Rev. Lett.* **1991**, *67*, 2355.
(54) Fedutik, Y.; Temnov, V. V.; Schöps, O.; Woggon, U.; Artemyev, M. V. Exciton-Plasmon-Photon Conversion in Plasmonic Nanostructures. *Phys. Rev. Lett.* **2007**, *99*, 136802.
(55) Hecker, N. E.; Höpfel, R. A.; Sawaki, N. Enhanced Light Emission from a Single Quantum Well Located near a Metal Coated Surface. *Phys. E (Amsterdam, Neth.)* **1998**, *2*, 98−101.
(56) Okamoto, K.; Niki, I.; Shvartser, A.; Narukawa, Y.; Mukai, T.; Scherer, A. Surface-Plasmon-Enhanced Light Emitters Based on Ingan Quantum Wells. *Nat. Mater.* **2004**, *3*, 601−605.
(57) Müller, R.; Malyarchuk, V.; Lienau, C. Three-Dimensional Theory on Light-Induced near-Field Dynamics in a Metal Film with a Periodic Array of Nanoholes. *Phys. Rev. B: Condens. Matter Mater. Phys.* **2003**, *68*, 205415.
(58) Ropers, C.; Park, D. J.; Stibenz, G.; Steinmeyer, G.; Kim, J.; Kim, D. S.; Lienau, C. Femtosecond Light Transmission and Subradiant Damping in Plasmonic Crystals. *Phys. Rev. Lett.* **2005**, *94*, 113901.
(59) Kim, D. S.; Hohng, S. C.; Malyarchuk, V.; Yoon, Y. C.; Ahn, Y. H.; Yee, K. J.; Park, J. W.; Kim, J.; Park, Q. H.; Lienau, C. Microscopic Origin of Surface-Plasmon Radiation in Plasmonic Band-Gap Nanostructures. *Phys. Rev. Lett.* **2003**, *91*, 143901−143901.
(60) Hamm, P. Coherent Effects in Femtosecond Infrared Spectroscopy. *Chem. Phys.* **1995**, *200*, 415−429.
(61) DeVoe, R. G.; Brewer, R. G. Observation of Superradiant and Subradiant Spontaneous Emission of Two Trapped Ions. *Phys. Rev. Lett.* **1996**, *76*, 2049.
(62) Akram, U.; Ficek, Z.; Swain, S. Decoherence and Coherent Population Transfer between Two Coupled Systems. *Phys. Rev. A: At., Mol., Opt. Phys.* **2000**, *62*, 013413.
(63) Zhu, S.; Scully, M. O. Spectral Line Elimination and Spontaneous Emission Cancellation Via Quantum Interference. *Phys. Rev. Lett.* **1996**, *76*, 388.



DOI: 10.1021/acsphotonics.5b00328
*ACS Photonics* 2015, 2, 1341−1347